ELSEVIER

Journal of Power Sources 81–82 (1999) 818–823

JOURNAL OF POWER SOURCES

www.elsevier.com/locate/jpowsour

FTIR and DEMS investigations on the electroreduction of chloroethylene carbonate-based electrolyte solutions for lithium-ion cells

M. Winter [a,*], R. Imhof [b], F. Joho [b], P. Novák [b]

[a] *Institute for Chemical Technology of Inorganic Materials, Graz University of Technology, Stremayrgasse 16 / III, A-8010 Graz, Austria*
[b] *Paul Scherrer Institute, Electrochemistry Section, CH-5232 Villigen PSI, Switzerland*

Abstract

Chloroethylene carbonate (ClEC) is decomposed to CO_2 at graphite electrodes. We assume that the CO_2 participates in the formation of an effective solid electrolyte interphase (SEI) on the electrode. Two in-situ techniques, subtractively normalized interfacial Fourier transform infrared spectroscopy (SNIFTIRS) and differential electrochemical mass spectrometry (DEMS), were applied in order to detect CO_2 formation and possible secondary reactions. The applied analytical methods provided conforming information about the onset of CO_2 formation (2.2–2.1 V vs. Li/Li^+).

Keywords: Lithium battery electrolyte; Chloroethylene carbonate; Graphite electrode; Solid electrolyte interphase; In-situ infrared spectroscopy; In-situ mass spectrometry

1. Introduction

Lithium batteries, in particular '4 V' lithium-ion cells, operate far beyond the thermodynamic stability window of the used organic electrolytes, and therefore, electrolyte decomposition occurs at the electrode/electrolyte interface. In order to evaluate the most suitable lithium battery electrolytes, the mechanisms and products of the electrolyte decomposition processes have been the subject of many investigations (see Refs. [1–6] and references cited therein). The electrolyte decomposition reactions depend on a large number of parameters like, e.g., (i) the composition of the electrolyte, (ii) both the type and surface properties of the electrode material, and (iii) the experimental electrochemical conditions during electrolyte decomposition. Moreover, these parameters can mutually affect each other which makes the analysis of the electrolyte decomposition processes very complex. We think that only the combined use of different analytical in-situ and ex-situ techniques can provide a sufficient basic knowledge to understand these processes.

In this paper, we use in-situ infrared spectroscopy and in-situ mass spectrometry to investigate the electroreduction of chloroethylene carbonate (ClEC)-based electrolytes at carbon electrodes. ClEC is one of only few known compatible electrolyte solvents that allow the use of graphite negative electrodes [7,8]. ClEC presumably forms a protective solid electrolyte interphase (SEI) [6] at the electrode/electrolyte interface which is permeable for Li^+ cations but almost impermeable for other electrolyte components. These SEI films prevent the co-intercalation of solvent molecules into the graphite matrix, a process which may result in an increased irreversible charge consumption and sometimes even in complete graphite exfoliation [2,5].

We have already shown by in-situ infrared spectroscopy that ClEC forms CO_2 during electrochemical reduction [8]. CO_2 is known for its beneficial influence on the SEI formation process [9]. In our preliminary experiments [8], bands of atmospheric CO_2 (*in* the IR beam but *outside* the electrochemical cell) superposed the infrared band of dissolved CO_2 in the electrolyte solution from ClEC decomposition, although the spectrometer was continuously purged with *dry, CO_2-free air*. Meanwhile, we have improved the experimental set-up by applying a very strict purging procedure of the spectrometer with *dry nitrogen*, which assures that the obtained IR spectra are not influenced by atmospheric CO_2 anymore. Additional and complementary information about the evolution of volatile reduction products has been achieved by differential electrochemical mass spectrometry (DEMS).

* Corresponding author. Tel.: +43-316-873-8268; Fax: +43-316-873-8272; E-mail: winter@ictas.tu-graz.ac.at

0378-7753/99/$ - see front matter
PII: S0378-7753(99)00116-0

2. Experimental

ClEC [Aldrich, 90% w/w, containing 10% w/w ethylene carbonate (EC)] was dried over lithiated molecular sieves for several weeks before use. EC (Selectipur, Merck, > 99.9%) was used as received. One molar electrolyte solutions of vacuum-dried $LiN(SO_2CF_3)_2$ (3 M, > 99.5%) were prepared, stored, and handled in an Ar-filled glove box (< 1 ppm H_2O). For the preparation of the 1 M $LiN(SO_2CF_3)_2$/EC electrolyte, the EC was slightly heated. The prepared EC electrolyte solution is liquid at ambient temperature. The water content of all electrolytes before the experiments was determined to be < 20 ppm by Karl–Fischer titration (Metrohm 684 KF Coulometer). All measurements were done at ambient temperature.

Cyclic voltammetric studies were performed in three electrode cells with lithium counter and reference electrodes [10]. Working electrodes were prepared by spraying a slurry of synthetic graphite TIMREX® SFG 6 (TIMCAL, Sins, Switzerland), polyvinylidene fluoride (PVDF, Aldrich), and 1-methyl-2-pyrrolidinone (Fluka) onto a titanium current collector. The electrodes were vacuum-dried at 120°C and contained ca. 10 mg of graphite (95% w/w SFG 6 + 5% w/w PVDF). The cyclic voltammograms (CVs) were performed at a scan rate of 0.01 mV s^{-1}.

In-situ subtractively normalized interfacial Fourier transform infrared spectroscopy (SNIFTIRS) [11] was performed with polished glassy carbon (GC) electrodes as described in Refs. [8,12]. After the beginning of the spectro-electrochemical experiment, the working electrode was kept at the reference potential of about 3 V vs. Li/Li^+ for 5 min and the reference spectrum, R_0, was measured. (The reference potential was the open circuit potential (OCP) of the electrode.) Next, the potential was decreased in steps of 0.1 V to 0.3 V vs. Li/Li^+ with an equilibration time of 5 min at each potential. During each equilibration, one spectrum R was measured. Further spectra were measured at open circuit after 5, 20, and 60 min, respectively, after switching off the current at 0.3 V vs. Li/Li^+. After the measurements, the water content of the electrolytes in the spectro-electrochemical cell was determined to be < 50 ppm.

In-situ DEMS was performed as described in Refs. [3,4]. The measurements were carried out under potentiodynamic conditions with a scan rate of 0.4 mV s^{-1}, using the open circuit potential of about 3 V as the starting point. The lower potential limit was 0.05 V vs. Li/Li^+.

3. Results and discussion

During electroreduction of a ClEC-based electrolyte [1 M $LiN(SO_2CF_3)_2$ in ClEC/EC (9:1), hereafter named ClEC:EC (9:1)], reductive currents negative to potentials of ~1.8 V vs. Li/Li^+ are observed on graphite electrodes (Fig. 1a). It follows from the comparison with a pure EC-based electrolyte (1 M $LiN(SO_2CF_3)_2$ in EC) (Fig. 1b) that this current peak is due to the presence of ClEC. This confirms previously reported data [8]. At the comparatively positive onset potential of ~1.8 V, the ClEC reduction products may form a protective SEI film before solvent co-intercalation occurs.

SNIFTIRS experiments on the ClEC/EC (9:1) electrolyte revealed the generation of CO_2 during reduction [8]. As an example, Fig. 2 shows a spectrum measured at 0.8 V vs. Li/Li^+. Positive bands represent a decrease in concentration and negative bands represent an increase in concentration of the species on the electrode and in the thin electrolyte layer between the electrode and the optical window. The sharp negative band at 2341 cm^{-1} was attributed to CO_2 formation *in the electrolyte* [14]. The CO_2 band has not been detected in analogous experiments in the pure EC-based electrolyte (see insert of Fig. 2). Moreover, according to the best of our knowledge, the reductive formation of CO_2 has not been reported for any other lithium battery electrolyte solvent so far.

In order to detect the onset potential of the electrochemical CO_2 formation, we evaluated the magnitude of the CO_2 band at ~2341 cm^{-1} vs. the potential (Fig. 3). According to the Lambert–Beer law, the concentration of a compound in the electrolyte sample is proportional to the

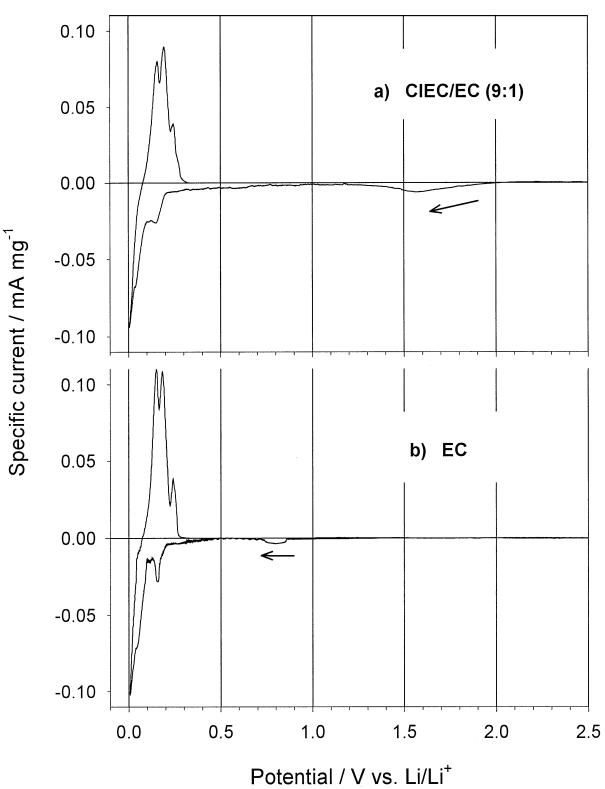

Fig. 1. Cyclic voltammograms of graphite TIMREX® SFG 6 in (a) 1 M $LiN(SO_2CF_3)_2$ in ClEC/EC (9:1), and (b) in 1 M $LiN(SO_2CF_3)_2$ in EC, scan rate = 0.01 mV s^{-1}.

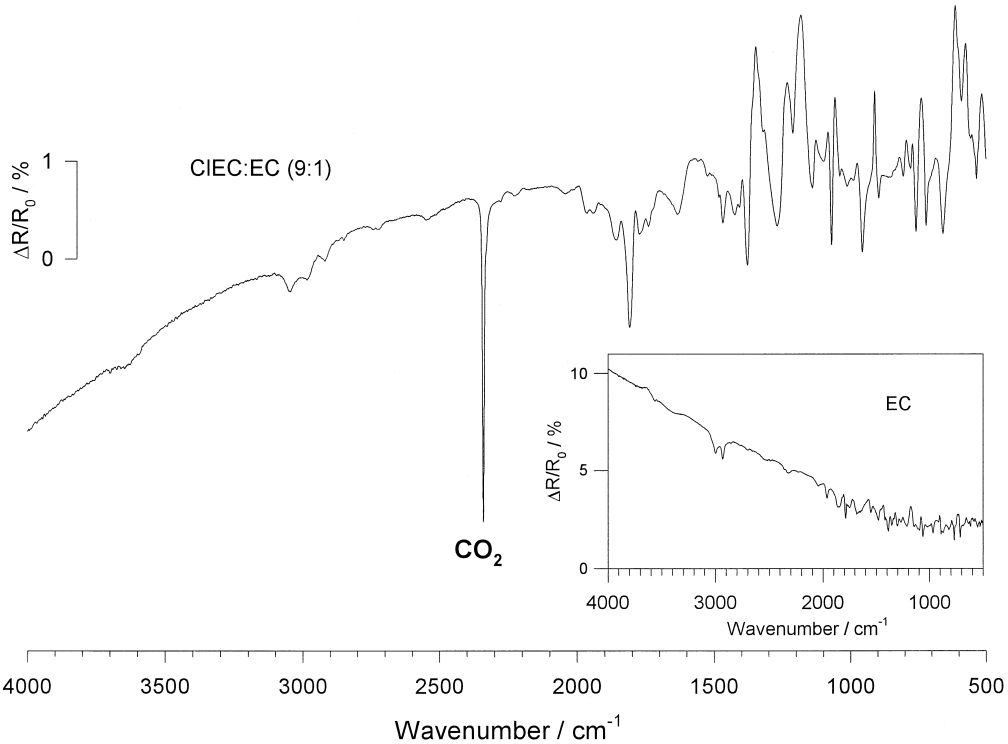

Fig. 2. The SNIFTIR spectrum measured on a polished GC electrode in 1 M $LiN(SO_2CF_3)_2$ in ClEC/EC (9:1); working potential: 0.8 V vs. Li/Li^+; reference potential: 3.1 V vs. Li/Li^+. The insert shows the SNIFTIR spectrum measured in 1 M $LiN(SO_2CF_3)_2$ in EC; working potential: 0.8 V vs. Li/Li^+; reference potential: 2.9 V vs. Li/Li^+.

measured absorbance. Therefore, the IR data recorded as reflectance were converted into absorbance units [13].

The onset potential of CO_2 formation was detected between 2.2 and 2.1 V vs. Li/Li^+ (see insert of Fig. 3), followed by a slight increase in CO_2 concentration between 2.1 V and 1.8 V vs. Li/Li^+. Below about 1.8 V a strong increase of CO_2 absorbance is observed which coincides with the beginning of the reductive current peak

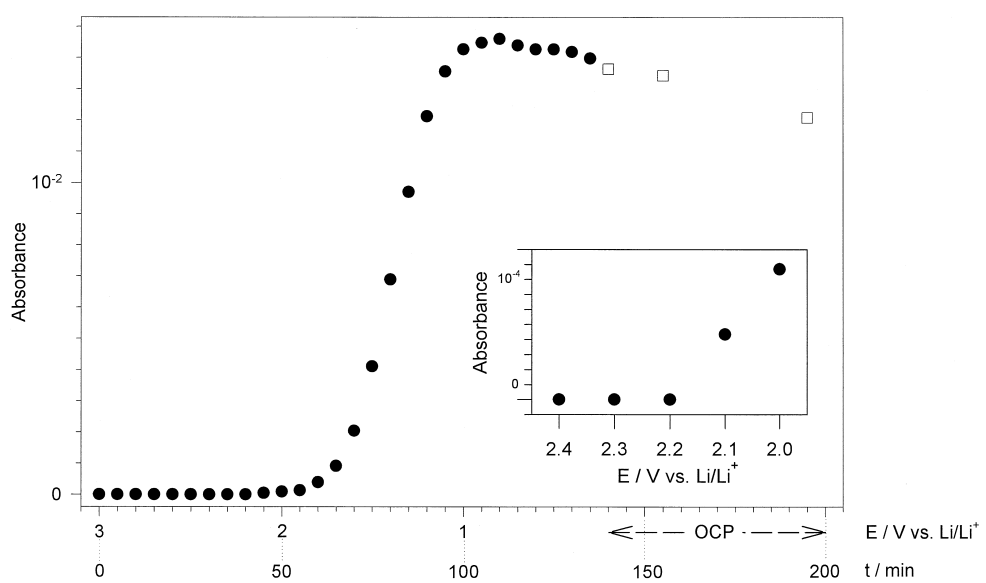

Fig. 3. CO_2 absorbance (at 2341 cm^{-1}) vs. potential of a polished GC electrode in 1 M $LiN(SO_2CF_3)_2$ in ClEC/EC (9:1); reference potential: 3.1 V vs. Li/Li^+. ●: taken from IR spectra recorded at the respective electrode potential, □: taken at OCP from IR spectra recorded after 5, 20, and 60 min, respectively, after switching off the current at 0.3 V vs. Li/Li^+. The insert shows a magnification of the potential region where the CO_2 evolution starts.

in the CV (Fig. 1a) and with the preliminary IR data we reported previously [8]. However, in the earlier experiments which were disturbed by atmospheric CO_2 in the spectrometer, we did not detect the small CO_2 absorption band between 2.2 and 1.8 V vs. Li/Li^+. The CO_2 absorbance reaches its maximum at 0.8 V vs. Li/Li^+ and gradually decreases at more negative potentials. We presume that the formed CO_2 contributes to the SEI formation. The spectra measured after the current was switched off at 0.3 V vs. Li/Li^+ showed that CO_2 diffuses away from the thin electrolyte layer between the electrode and the optical window (Fig. 3).

Apart from SNIFTIRS, DEMS is a valuable technique to detect all kinds of gaseous or volatile reaction products. The currents in the CVs (a) as well as the mass signals (MSCV) for the masses $m/z = 2$ (b), 27 (c), and 44 (d), which represent hydrogen, ethylene, and CO_2, respectively, were recorded simultaneously as a function of the potential (Fig. 4). The reductive behavior of pure EC, which is the main contaminant in the ClEC:EC (9:1) electrolyte, was monitored for comparison reasons.

The CVs of the two electrolytes differ considerably (Fig. 4a). In the case of EC, one observes reductive and oxidative current peaks corresponding to the intercalation/

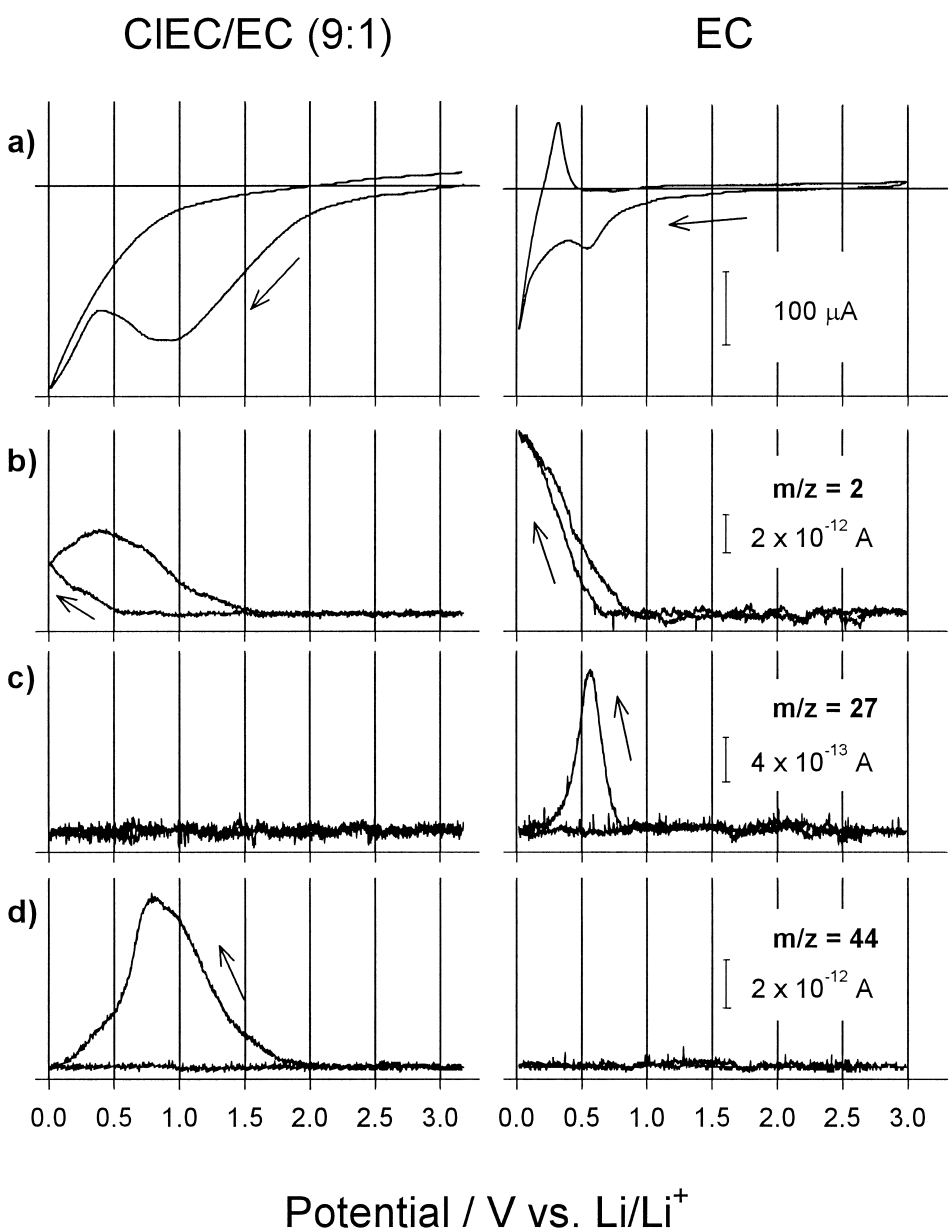

Fig. 4. CV (a) and MSCV (b, c, d) of graphite TIMREX® SFG 6 in 1 M $LiN(SO_2CF_3)_2$ in ClEC/EC (9:1) (left) and 1 M $LiN(SO_2CF_3)_2$ in EC (right). The MSCVs show $m/z = 2$ (b), $m/z = 27$ (c), and $m/z = 44$ (d), representing hydrogen, ethylene, and CO_2, respectively.

de-intercalation of lithium ions into the graphite. In contrast, the ClEC/EC (9:1) mixture shows poor reversibility. Several reasons should be considered to explain this behavior:

Scan rate. The DEMS measurements were performed at a relatively high scan rate of 0.4 mV s^{-1}. Due to kinetic effects, the coulombic efficiency of the intercalation/de-intercalation process in both electrolytes is therefore rather low in comparison to voltammetric experiments with a slower scan rate (cf. Fig. 1, where at a scan rate of 0.01 mV s^{-1}, good reversibility can be observed).

Lithium ion transfer through the SEI. It is possible that films formed in the presence of neat EC allow a faster lithium ion intercalation/de-intercalation than the films formed in the ClEC:EC (9:1) electrolyte. This agrees with the results of Fig. 1 where sharper intercalation and de-intercalation peaks in the case of the EC electrolyte reveal faster kinetics.

Removal of CO_2 from the electrochemical cell. In general, one has to be aware that the concentration of volatile compounds in the electrolyte may change during the DEMS experiment. In our case, the vacuum pump exhausts some CO_2 formed in the ClEC:EC (9:1) electrolyte. The amount of CO_2 in the electrolyte is therefore reduced and, thus, may be insufficient for effective film formation on the graphite electrode.

The mass signals in the DEMS experiment (Fig. 4) behaved as anticipated. In accordance with the IR experiment (Fig. 3), the beginning of the CO_2 evolution from ClEC:EC (9:1) was detected at about 2.1 V vs. Li/Li^+. It reaches a maximum at $\sim$0.8 V vs. Li/Li^+ in the DEMS experiment and vanishes at a potential of $\sim$0.1 V vs. Li/Li^+. For pure EC, at the first scan, we found ethylene evolution at potentials negative to about 0.8 V vs. Li/Li^+ (Fig. 4c, right). According to Besenhard et al. [5], the corresponding current peak between 0.8 and 0.4 V vs. Li/Li^+ is attributed to solvent co-intercalation and subsequent SEI film formation. In contrast, in the presence of ClEC, the EC in the electrolyte blend behaves differently, since no ethylene is observed over the whole potential region. In the ClEC:EC (9:1) electrolyte, the SEI (probably already formed at potentials below 2.0 V vs. Li/Li^+, cf. Fig. 1) and/or other decomposition products of ClEC may hinder the electrochemical decomposition of EC and/or change its decomposition mechanism. As a result, the possible co-intercalation of EC into graphite seems to be prevented and no ethylene gas is detected in the presence of ClEC.

In both electrolyte solutions, hydrogen is evolved below $\sim$0.6 V vs. Li/Li^+ (Fig. 4). This agrees with our previous observations for an EC/DMC electrolyte [4]. The origin of the hydrogen is unknown. It might originate from (i) the trace water in the cell, (ii) hydrogen-containing surface groups of the graphite like C–OH, COOH, and C–H, and (iii) the electrolyte solvents or their decomposition products.

We finally emphasize that both in-situ methods show the same results regarding the detection of CO_2, although different electrodes, GC in the SNIFTIRS measurements and graphite in the DEMS measurements, have been employed. This indicates that the surface of a GC electrode may serve as a model of the surface of practical graphite electrodes to some extent.

4. Conclusion

During electroreduction on carbon electrodes, ClEC electrolytes evolve CO_2. Both in-situ DEMS and SNIFTIRS measurements confirm that CO_2 is formed at potentials below 2.2 V vs. Li/Li^+. First, the amount of CO_2 in the electrolyte increases slowly. However, at potentials negative to $\sim$1.8 V vs. Li/Li^+, a large amount of CO_2 is evolved which correlates well with the occurrence of a broad current peak in the potentiodynamic experiments. Furthermore, DEMS results reveal that also hydrogen is formed during the electroreduction reaction.

Acknowledgements

This work was partially supported by the Swiss Federal Office of Energy, Bern, and the Austrian Science Fund. We are grateful to Dr. M.E. Spahr, TIMCAL AG, Sins, Switzerland, for the donation of the graphite samples and Dr. O. Haas (Paul Scherrer Institute) and Prof. J.O. Besenhard (Graz University of Technology) for useful discussions.

References

[1] L.A. Dominey, in: G. Pistoia (Ed.), Lithium Batteries: New Materials, Developments and Perspectives, Chap. 4, Elsevier, Amsterdam, 1994.
[2] M. Winter, J.O. Besenhard, M.E. Spahr, P. Novák, Adv. Mat. 10 (1998) 725.
[3] R. Imhof, P. Novák, in: C.F. Holmes, A.R. Landgrebe (Eds.), Batteries for Portable Applications and Electric Vehicles, Proceedings Volume PV 97-18, The Electrochemical Society, Pennington, NJ, 1997, p. 313.
[4] R. Imhof, P. Novák, J. Electrochem. Soc. 145 (1998) 1081.
[5] J.O. Besenhard, M. Winter, J. Yang, W. Biberacher, J. Power Sources 54 (1995) 228.
[6] E. Peled, D. Golodnitzky, G. Ardel, J. Electrochem. Soc. 144 (1997) L208.
[7] Z.X. Shu, R.S. McMillan, J.J. Murray, I.J. Davison, J. Electrochem. Soc. 143 (1996) 2231.
[8] M. Winter, P. Novák, J. Electrochem. Soc. 145 (1998) L27.

[9] J.O. Besenhard, P. Castella, M.W. Wagner, Mater. Sci. Forum 91–93 (1992) 647.
[10] P. Novák, W. Scheifele, F. Joho, O. Haas, J. Electrochem. Soc. 142 (1995) 2544.
[11] S. Pons, J. Electroanal. Chem. 150 (1983) 495.
[12] F. Joho, PhD Thesis No. 11745, ETH Zürich, Switzerland, 1996.
[13] M. Spiekermann, in: B. Schrader (Ed.), Infrared and Raman Spectroscopy, Chap. 5.1, VCH, Weinheim, 1995, p. 413.
[14] P. Novák, P.A. Christensen, T. Iwasita, W. Vielstich, J. Electroanal. Chem. 263 (1989) 37.